

# SCIENTIFIC REPORTS



OPEN

## Cloning and characterization of farnesyl pyrophosphate synthase from the highly branched isoprenoid producing diatom *Rhizosolenia setigera*

Received: 27 October 2014

Accepted: 07 April 2015

Published: 21 May 2015

Victor Marco Emmanuel N. Ferriols<sup>1,2</sup>, Ryoko Yaginuma<sup>1</sup>, Masao Adachi<sup>3</sup>, Kentaro Takada<sup>1</sup>, Shigeki Matsunaga<sup>1</sup> & Shigeru Okada<sup>1</sup>

The diatom *Rhizosolenia setigera* Brightwell produces highly branched isoprenoid (HBI) hydrocarbons that are ubiquitously present in marine environments. The hydrocarbon composition of *R. setigera* varies between C<sub>25</sub> and C<sub>30</sub> HBIs depending on the life cycle stage with regard to auxosporulation. To better understand how these hydrocarbons are biosynthesized, we characterized the farnesyl pyrophosphate (FPP) synthase (FPPS) enzyme of *R. setigera*. An isolated 1465-bp cDNA clone contained an open reading frame spanning 1299-bp encoding a protein with 432 amino acid residues. Expression of the RsFPPS cDNA coding region in *Escherichia coli* produced a protein that exhibited FPPS activity *in vitro*. A reduction in HBI content from diatoms treated with an FPPS inhibitor, risedronate, suggested that RsFPPS supplies precursors for HBI biosynthesis. Product analysis by gas chromatography-mass spectrometry also revealed that RsFPPS produced small amounts of the *cis*-isomers of geranyl pyrophosphate and FPP, candidate precursors for the *cis*-isomers of HBIs previously characterized. Furthermore, RsFPPS gene expression at various life stages of *R. setigera* in relation to auxosporulation were also analyzed. Herein, we present data on the possible role of RsFPPS in HBI biosynthesis, and it is to our knowledge the first instance that an FPPS was cloned and characterized from a diatom.

Diatoms are one of the most ecologically diverse groups of organisms in today's oceans with estimates ranging from 30,000 to 100,000 species<sup>1</sup>, all of which play a major role in supporting higher trophic levels and carbon fluxes in marine ecosystems<sup>2</sup>. Despite the extensive diversity of this group, only a handful of species have been found to produce structurally unique C<sub>25</sub> and C<sub>30</sub> highly branched isoprenoid (HBI) hydrocarbons<sup>3</sup>. These HBIs are of great interest given that they have been extensively used as geochemical markers in marine sediments due to their ubiquitous nature<sup>4</sup>, and that some of the C<sub>25</sub> HBIs have also been found to exhibit cytostatic effects on certain lung cancer cell lines<sup>5</sup>. The unique branched structure of these HBIs also make them a potential form of biofuel through a hydrocracking process similar to botryococcene isoprenoids from the freshwater alga *Botryococcus braunii*<sup>6,7</sup>.

Among the handful of diatoms that produce these unique HBIs, *Rhizosolenia setigera* has garnered considerable attention since this species was found to produce a variety of isomers of both C<sub>25</sub> and C<sub>30</sub> HBIs depending on the strain, culture conditions, and position in its life cycle<sup>5,8,9</sup>. Masse and co-workers<sup>10</sup> established that the HBIs produced by *R. setigera* are mainly produced by the mevalonate (MVA) pathway

<sup>1</sup>Graduate School of Agricultural and Life Sciences, The University of Tokyo, Japan. <sup>2</sup>Institute of Aquaculture, University of the Philippines Visayas, Philippines. <sup>3</sup>Faculty of Agriculture, Kochi University, Japan. Correspondence and requests for materials should be addressed to S.O. (email: aokada@mail.ecc.u-tokyo.ac.jp)

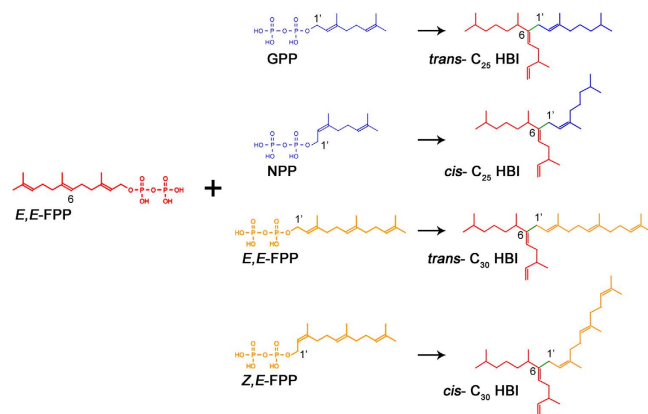


**Figure 1.** Simplified hypothetical biosynthetic pathway for the formation of representative C<sub>25</sub> and C<sub>30</sub> highly branched isoprenoids produced by *R. setigera*. Red structures (*E,E*-FPP) represent the C<sub>15</sub> isoprenoid unit to which a C<sub>10</sub> (blue structures, GPP or NPP) or another C<sub>15</sub> (orange structures, *E,E*-FPP or *Z,E*-FPP) isoprenoid unit attaches at C-6 to produce the *trans*- or *cis*- forms of C<sub>25</sub> and C<sub>30</sub> HBIs respectively through 1'-6 coupling. Biosynthetic scheme is patterned after those proposed in previous studies (Masse *et al.*, 2004b; Belt *et al.*, 2006).

for isoprenoid biosynthesis through a series of experiments using isotopic labeling techniques. Despite this, the study was only limited to using substrates that were utilized in more upstream processes of the MVA pathway (isotopically labeled acetate, glucose, and CO<sub>2</sub>), and the final steps in the actual synthesis of these hydrocarbons still remain to be elucidated. It has been suggested that the C<sub>25</sub> and C<sub>30</sub> HBIs are formed by the attachment of a C<sub>10</sub> or C<sub>15</sub> isoprenoid unit respectively at C-6 of another C<sub>15</sub> isoprenoid unit to produce the unique T branch point observed in their structures<sup>11,12</sup>. Farnesyl pyrophosphate (FPP) produced by FPP synthase (FPPS) (EC 2.5.1.10) is the most promising candidate for the C<sub>15</sub> unit used for the formation of HBIs (Fig. 1).

FPPS is an enzyme that catalyzes the head to tail condensation of two molecules of isopentenyl pyrophosphate (IPP) with dimethylallyl pyrophosphate (DMAPP)<sup>13</sup> to form FPP. FPP is subsequently converted into a wide range of other natural products such as squalene (through the coupling of two FPP molecules via squalene synthase)<sup>14</sup>, 5-*epi*-aristolochene (through the cyclization of FPP via 5-*epi*-aristolochene synthase)<sup>15</sup>, and other volatile sesquiterpenes such as β-farnesene and α-bergamotene<sup>16</sup>. FPP also plays an important role in the prenylation of proteins wherein protein prenyltransferases catalyze the addition of the carbon moiety of FPP to a cysteine residue in the CaaX motif of a target protein, thus facilitating the functional anchoring of these proteins to cell membranes<sup>17</sup>. cDNA cloning of FPPS has already been carried out from a wide range of organisms such as human<sup>18</sup>, rat<sup>19</sup>, yeast<sup>20</sup>, and higher plants<sup>21–23</sup>, and several studies have also highlighted the important regulatory function of this enzyme in producing precursors and substrates for more complex essential metabolites<sup>24–26</sup>.

In the context of *R. setigera*, FPPS presents an interesting research target assuming that a C<sub>15</sub> isoprenoid unit is used as one of the precursors for the production of C<sub>25</sub> and C<sub>30</sub> HBIs. Therefore, the aim of this study was to clone and characterize a potential FPPS cDNA from *R. setigera*, to seek a possible role of the enzyme encoded by this cDNA as the supplier of precursors for HBI biosynthesis, and to determine changes in its gene expression in relation to the position of *R. setigera* in its life cycle. Furthermore, it is to our knowledge the first instance that an FPP synthase was cloned and characterized from the extensively diverse diatoms.

## Results

**Isolation of RsFPPS cDNA.** A tentative FPPS cDNA was isolated from *R. setigera* CCMP1694 through a series of bioinformatics and PCR techniques. Using amino acid sequences of known FPP synthases as local BLAST queries and limiting the expectation value [E] of the local BLAST function on BioEdit (V 7.2.3) to 1 × 10<sup>-6</sup>, a single contig was identified from each of the independent *R. setigera* EST databases from Kochi University and the University of Tokyo. One contig corresponded to 1545 bp while the other corresponded to 1474 bp. Both contigs contained a putative open reading frame (ORF) corresponding to 1299 bp (RsFPPS) with 100% identity to each other and encoding 432 amino acids. Using primers designed from these contig sequences, a 1465 bp fragment was amplified by PCR and cloned as the plasmid pBs-RsFPPS1465. This clone contained an ORF of 1299 bases preceded by 21 bases of 5'-UTR and followed by 145 bases of 3'-UTR (Fig. S1).

**Comparison of RsFPPS against FPPS from other organisms.** The predicted molecular weight of *R. setigera* FPPS is 48.94 kDa, which falls within the range for those from mammals (~48 kDa)<sup>27,28</sup>, and is relatively larger than those from plants and fungi (39–44 kDa)<sup>20–22,29</sup>, and bacteria (~32 kDa)<sup>30</sup>. A BLAST

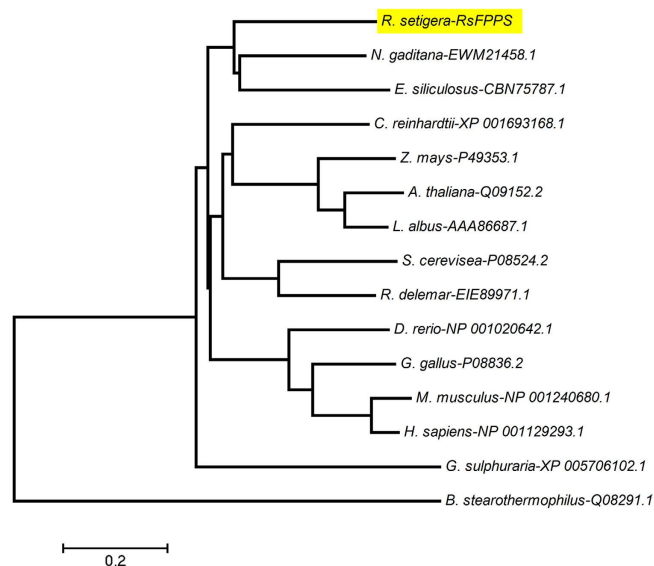


**Figure 2. FPPS phylogenetic tree.** *R. setigera* FPPS was compared against those from animal, plant, yeast, algae, and bacteria sources using the Neighbor Joining method based on their amino acid sequences. Alphanumeric codes to the right of the binomial names correspond to accession numbers on the NCBI database. The scale bar on the bottom-left is representative of the degree of difference among sequences wherein a distance of 0.2 infers a 20% difference among sequences.

search against the NCBI online protein database showed that the deduced RsFPPS amino acid sequence shared 58% and 55% identity with annotated FPPSs from eustigmatophytes and brown algae, respectively, and 46–51% identity with representative FPP synthase sequences from other organisms (animals, higher plants, green algae, and fungi). Phylogenetic analysis of RsFPPS showed that it was more closely related to algal FPP synthase than to those of animals, higher plants, fungi, or bacteria based on sequence conservation (Fig. 2). Sequence alignment of the putative amino acid sequence of RsFPPS against those of mammals, plants, yeast, and bacteria (Fig. 3) revealed that it contained all conserved amino acid residues necessary for substrate binding and catalytic activity (domains I–VII) typical of other identified FPPSs<sup>31</sup>. Two characteristic aspartate-rich motifs were also present in the RsFPPS sequence (Fig. 3).

**Purification of RsFPPS protein expressed in *E. coli*.** The nucleotide sequence corresponding to the open reading frame of RsFPPS (of which the ATG start codon was removed) was inserted into the pET200/D-TOPO expression vector (pET200-RsFPPS1296) and transformed into BL21(DE3) *E. coli* cells. Under the conditions described in *Supplementary Methods*, appreciable amounts of the recombinant protein were obtained as soluble proteins for Ni-NTA purification.

Recombinant RsFPPS, which had an approximate size of 53 kDa due to the inclusion of a 6x-His tag and a linker sequence from the pET200/D-TOPO vector, was isolated to near purity as determined by SDS-PAGE (Fig. S2). The purified protein preparation showed detectable enzyme activity when incubated with IPP and DMAPP or geranyl pyrophosphate (GPP) as seen in the formation of GPP and FPP from liquid chromatography-mass spectrometry (LC/MS) analysis of the reaction mixtures (Fig. 4A,B). Therefore, the *R. setigera* RsFPPS was found to encode for a functional FPPS enzyme.

**Product analysis by LC/MS and enzyme kinetics.** An LC/MS assay was established to reproducibly identify FPPS reaction products. LC/MS analysis for the detection and quantification of GPP and FPP standards prepared in sample matrices identical to those used for enzyme assays provided sensitive and reproducible results at concentrations ranging from 0.5 to 250  $\mu$ M. Sufficient separation of GPP and FPP was achieved with sharp peaks of GPP and FPP at retention times of 4.0 and 4.9 min respectively (Fig. 4C). Identification of RsFPPS reaction products (GPP and FPP) was confirmed by similar retention times (Fig. 4A,B) and mass spectra (Fig. S3) to those of the standards used. This allowed for the determination of steady state enzyme kinetics for RsFPPS, wherein enzyme activity was computed as the amount of FPP molecules formed per min per mg protein.

Varying concentrations of the substrates IPP, DMAPP, and GPP were used to determine the steady state kinetic constants for recombinant RsFPPS (Fig. 5A–D). For reactions where the IPP concentration was kept constant (50  $\mu$ M) and DMAPP or GPP were used as counter substrates, the  $K_m$  value for DMAPP was 6-fold lower than the derived  $K_m$  value for GPP (Fig. 5A,C). In parallel reactions where the DMAPP (50  $\mu$ M) or GPP (100  $\mu$ M) concentrations were kept constant and IPP was used as a counter substrate,  $K_m$  values for IPP did not differ significantly (Fig. 5B,D). It was noted though, that at higher

<i>R. setigera</i>	MVSSLPPIIAGAAIYRLVSSKTLPLDLSAFFELEIPDQISLLSLLFASVFSVAVSISGFIAPPGHNDDEDEHKPPFYQP	80
<i>M. musculus</i>	--MPLSCWLRSLGVFLLPAPCWAP--RERWLGFLQRPSTLAYGCPVLGAWHSARWVCQVWTEEPRAFSSSVRMNGN----	71
<i>L. albus</i>	-----	1
<i>Z. mays</i>	-----	5
<i>A. thaliana</i>	-----MSVSCCCRNLGKTIKKAIPSHHLHLRSLGGSLYRRR	36
<i>S. cerevisiae</i>	-----MASE-----	4
<i>B. stearothermophilus</i>	-----	1
<b>Consensus</b>		
I		
<i>R. setigera</i>	LKEIASKTITDKEKFLSVYPCLRDSIAEYFATKHEMVPEGVNWTIMIDYSCV--GKMNRGITVLTIVARTLSGS--SGLTP	157
<i>M. musculus</i>	--QKLDAYNQEKQNFQIFHSQIVKVLTEK--ELGHP EIGDAIARLKEVLEYNAL--GKYNRGLTVVQAFQELVEP--KKQDA	146
<i>L. albus</i>	-----MADLRSTFLNVYSVLKSELLH--DPAFEFSPDSRQWLDRLMDYNVP--GGKLNRLSVIDSYRLLKDG--HELND	69
<i>Z. mays</i>	-----NGAGGDTRAAAFARIYKTLKEELLT--DPAFEFTEESRQWIDRMVDYNVL--GGKCNRLSVDVSYKLLKGA--DALGE	77
<i>A. thaliana</i>	IQSSSMEIDLKSTFLNVYSVLKSDLLH--DPSFEFTNESRLWVDRMLDYNVR--GGKLNRLSVDVSYKLLKQG--NDLTE	111
<i>S. cerevisiae</i>	--KEIR-----RERFLNVFPKLV EELNASLLA--YGMPEACDWAYHSLNYNTP--GGKLNRLSVDVSYKLLKQG--NDLTE	76
<i>B. stearothermophilus</i>	-----MAQLSVEQFLNEQKQAVETALSR--YIERLEGPAKLLKAMAYSLEAGGKRIRPLLLSTVRALGKD-----	64
<b>Consensus</b>	F Y G G K R L	
II III		
<i>R. setigera</i>	REEARASVVGWGI EFLQAFFLVA DDL--MDSKTRRGQPCWYLLPKVGTIAVNDSFLESFVFTFLKEHFGKEPYIYIKLV	235
<i>M. musculus</i>	ESLQRALTVGWCVELLQAFFLVS DDI--MDSLTRRGQICWYQKPGIGLDAINDALLEASIRLLKFKYCREQPYLNL	224
<i>L. albus</i>	DEIFLASALGWCI EWLQAYFLV LDDI--MNSHTRRGQPCWFRVVPKVMIAANDGVLLRNH IPRILKKHFRGKPYADLL	147
<i>Z. mays</i>	EETFLACTL GWCI EWLQAFFLVL DDI--MDSHTRRGQPCWFRVVPQVGLIAANDGIILRNHISRILRRHFRGKPYADLL	155
<i>A. thaliana</i>	QEVFLSCALGWCI EWLQAYFLV LDDI--MNSVTRRGQPCWFRVVPQVGMVAINDGILLRNH IHRILKKHFRDQKPYVDLV	189
<i>S. cerevisiae</i>	EEYEKVA I L GWCI EWLQAYFLV LDDM--MDSITRRGQPCWYKVEVGEI AINDAFMLEAAIYKLLKSHFRNEKYYIDIT	154
<i>B. stearothermophilus</i>	--PAVGLPVACAIEMIHTYSLIH DDLPSMDNDDLRRGKPTNHKVFGEAMAILAGDGLLTYAFQLITEIDDERIPPSVRLR	142
<b>Consensus</b>	E L D D M D R R G L	
IV V		
<i>R. setigera</i>	ELFLETIQQTEC---GQLLDLTSQPKDAKTADLSRFTIERYRKIVKYKTA FYSFYLPVAVASMLMSGVNTSKSFKTARNI	311
<i>M. musculus</i>	DLFLQSSYQTEI---GQTLDMTAPQGHV--DLGRYTEKRYKSI VKYKTA FYSFYLPVIAAAMYAGIDGKEHANALKI	298
<i>L. albus</i>	DLFNEVEFQTAS---GQMIDLITLLEGEK--DLSKYTSLSHRRIVQYKTA FYSFYLPVACALLMVG E--NLDNHIDVKN I	220
<i>Z. mays</i>	DLFNEVEFQTAS---GQLLDLITLLEGEK--DLTKYNITVHGRIVQYKTA FYSFYLPVACALLSSE--NLDNYGDVENI	228
<i>A. thaliana</i>	DLFNEVELQTAC---GQMIDLITLLEGEK--DLAKYSLSIHRRIVQYKTA FYSFYLPVACALLMAGE--NLENHIDVKNV	262
<i>S. cerevisiae</i>	ELFHVEVTFQTEL---GQLMDLITAPEDK--VDLSKFS LKKS HSFIVT FKTAYYSFYLPVALAMYVAGITDEKDLKQARDV	228
<i>B. stearothermophilus</i>	LIERLAKAAGPEGMVAGQAADMEGEG-----KTLTLESELYIHRHKTGKMLQYS--VHAGALIGGA--DARQTRELDEF	212
<b>Consensus</b>	G Q D I K T Y G	
VI		
<i>R. setigera</i>	CCIMGEYFQIQDDVLLCYGTP E VIGK--VGTDIQDNKCSWLIVQALDRATPEQRKVI EENY GKWDDAKVAKIKAIYNEMGL	390
<i>M. musculus</i>	LMEMGEFFQVQDDYLLDFGDP SVTGK--VGTDIQDNKCSWLIVVQCLLRAS PQQRQILEENY GQKDPKVARVKALYEALDL	377
<i>L. albus</i>	LVDMGTYFQVQDDYLLDFGAPETIGK--IGTDIEDFKCSWLIVVQALERADESQKRILFENY GKKDPANVAKVKALYDELNL	299
<i>Z. mays</i>	LVEMGTYFQVQDDYLLDFGDP EFIGK--IGTDIEDYKCSWLIVVQALERADESQKRILFENY GKKDPACVAKVKALYKELDL	307
<i>A. thaliana</i>	LVDMGTYFQVQDDYLLDFADPETL GK--IGTDIEDFKCSWLIVVQALERCSEEQT KILYENY GKKDPSPNAVAKVKALYKELDL	341
<i>S. cerevisiae</i>	LIPLGEYFQIQDDYLLDFGTP E QIGK--IGTDIQDNKCSWVINKALELASAEQRKTLDENY GKKDSVAEAKCKKI FNDLKI	307
<i>B. stearothermophilus</i>	AAHLGLAFQIRDDILDIEGAEKIGKPVGSDQSNNKATYPALLSLAGAKEKLAFHIEA-----AQRHLRNADV	280
<b>Consensus</b>	G F Q D D L D G K G D K L	
VII		
<i>R. setigera</i>	KSVFEKY EEDSYAEIQEELK KIND---IPQEVFTLFLDKIYKRSK--	432
<i>M. musculus</i>	QSAFFKY EEDSYNRLKSLIEQCSAP--LPPSIFMELANKIYKRRK--	420
<i>L. albus</i>	QGVFTIYESKSYEKLVTISIEAHP S--KAVQALLKSF LKGIYKRQKL	343
<i>Z. mays</i>	EAVFQ EYENESYKLIADIEAQPS--IAVQKVLKSF LHKIYKRQK--	350
<i>A. thaliana</i>	EGVFMEYESKSYEKLGAIEGHQS--KAIQAVLKSFLAKIYKRQK--	384
<i>S. cerevisiae</i>	EQLYHEYEESI AKDLKAKISQVDES RGFKADVLTAF LNKYKRSK--	352
<i>B. stearothermophilus</i>	DGAALAYICELVAARDH-----	297
<b>Consensus</b>	Y	

**Figure 3. Multiple amino acid sequence alignment of *R. setigera* FPPS.** Comparisons were made against those from mouse, yeast, bacteria, and plants. Conserved domains typical of FPP synthases are marked by Roman numerals (I-VII) and a bar above the sequences. The first and second aspartate rich regions in domains II and VI respectively are indicated by boxes.

concentrations of IPP (200  $\mu$ M), decreases in enzyme activity were observed. Because of this observation, the enzyme-inhibitor constant ( $K_i$ ) for substrate inhibition in these set of reactions was determined, and it revealed that reactions with DMAPP had around two-fold higher  $K_i$  values for IPP than reactions with GPP (Fig. S5). Conversely, in terms of the turnover rate ( $k_{cat}$ ) of RsFPPS, reactions where GPP was used as the counter substrate (Fig. 5C,D) showed  $k_{cat}$  values that were 10-fold higher compared to reactions with DMAPP as the counter substrate (Fig. 5A,B), indicating that FPP is more efficiently produced when GPP is used as its allylic substrate.

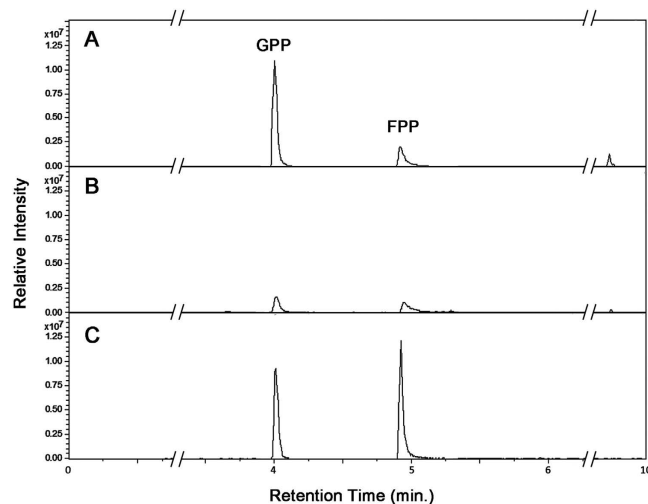


**Figure 4. Representative LC/MS extracted ion chromatograms (EIC).** A) Enzyme reaction with IPP and GPP as substrates, B) enzyme reaction with IPP and DMAPP as substrates, C) GPP and FPP standards at 100  $\mu\text{M}$  concentrations. GPP and FPP eluted at retention times of 4.0 and 4.9 minutes respectively.

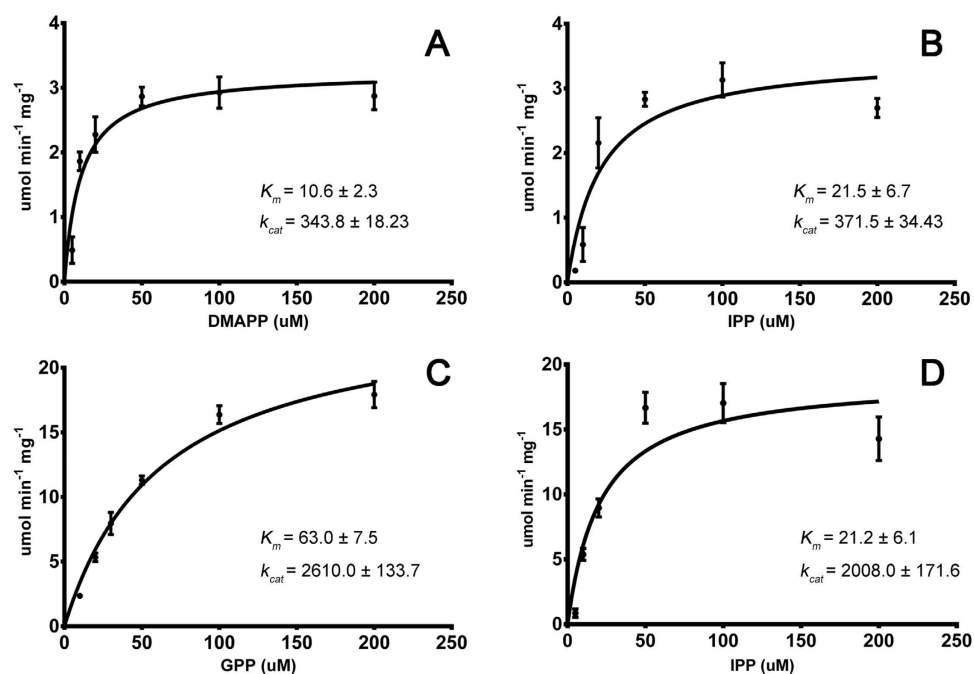


**Figure 5. RsFPFS enzyme kinetics.** Purified recombinant RsFPFS was subjected to enzyme assays to determine the effect of varying concentrations of the allylic substrates A) DMAPP and C) GPP on enzyme activity. Parallel reactions using IPP as the counter substrate against B) DMAPP (50  $\mu\text{M}$ ) and D) GPP (100  $\mu\text{M}$ ) were also conducted. Inset values (A-D) are the means ( $\pm$ S.D.) of the derived kinetic constants  $K_m$  ( $\mu\text{M}$ ) and  $k_{cat}$  ( $\text{min}^{-1}$ ). Values for  $k_{cat}$  were calculated using the dimeric form of the enzyme.

**Product analysis by gas chromatography/mass spectroscopy (GC/MS).** Products of large scale enzyme assays using IPP and DMAPP as substrates were further verified by GC/MS after converting the generated prenyl pyrophosphates to their corresponding alcohols using alkaline phosphatase. This was done in order to check for possible formation of reaction product *cis*-isomers since separation of GPP and FPP *cis*- and *trans*-isomers was difficult using the described LC/MS conditions. The formation of geraniol (GOH) and *E,E*-farnesol (*E,E*-FOH) was easily detected by GC/MS with peaks appearing at retention times of 12.45 and 18.45 min, respectively (Fig. 6A,B, upper panels; Fig. S4). Interestingly, small amounts of their *cis*- isomers, nerol (NOH) and *Z,E*-farnesol (*Z,E*-FOH), were also detected with retention times of 12.12 and 18.22 min, respectively (Fig. 6A,B, lower panels; Fig. S4). When IPP and

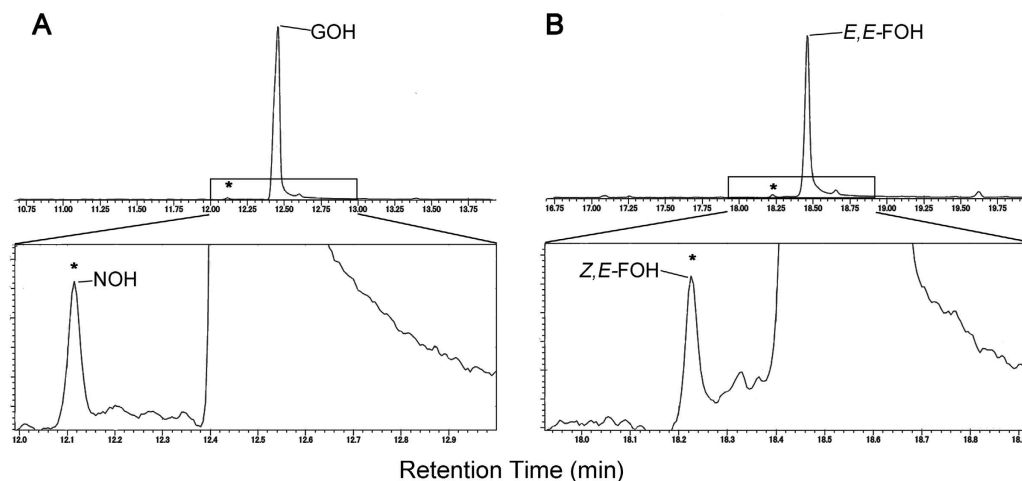


**Figure 6.** GC/MS total ion chromatogram of enzyme reaction products using IPP and DMAPP as substrates. Upper panels show prominent peaks corresponding to A) geraniol (GOH) and B) *E,E*-farnesol (*E,E*-FOH) with minor peaks for nerol (NOH) and *Z,E*-farnesol (*Z,E*-FOH) marked with asterisks (\*). Lower panels are magnified images of the boxed areas in the upper panels. Other minor peaks in the upper panels are either contaminants or artefacts of treatment with alkaline phosphatase as determined in control alkaline phosphatase reactions using GPP or *E,E*-FPP standards.

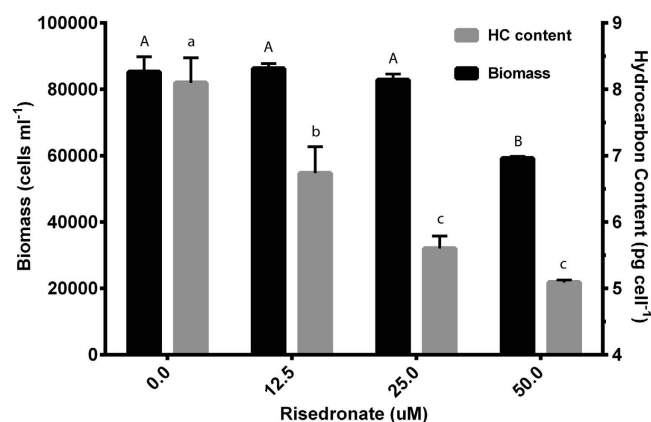


**Figure 7.** Effect of risedronate on the growth and hydrocarbon content of *R. setigera*. Biomass of *R. setigera* after two-day incubation with risedronate is presented as cells ml<sup>-1</sup>. Total HBI content of *R. setigera* quantified by GC/MS is presented as pg cell<sup>-1</sup>. Values under different letters denote significant differences ( $p < 0.05$ ) with capital and small letters corresponding to biomass and hydrocarbon content data respectively.

GPP were used as substrates, only a small amount of *Z,E*-FOH was detected and no peak corresponding to NOH was observed. The peaks for the *cis*-isomers were not detected when control reactions using GPP and *E,E*-FPP standards were treated with alkaline phosphatase indicating that the expressed RsFPPS produced a small amount of neryl pyrophosphate (NPP) and *Z,E*-FPP as minor products.

**Inhibition of HBI production in diatoms treated with an FPPS-specific inhibitor.** Upon observing that RsFPPS produces potential precursors for HBI biosynthesis, we conducted further experiments to assess how RsFPPS inhibition would affect overall hydrocarbon production. *R. setigera* cultures fifteen cycles after an auxosporulation event (which were mainly producing C<sub>25</sub> HBIs) were subjected to doses of the FPPS-specific inhibitor risedronate in a range from 0 to 50 μM after a 4-day pre-incubation period (Fig. 7). In terms of overall growth, risedronate did not have a significant effect on the final biomass (cells•ml<sup>-1</sup>) of treated cells for concentrations up to 25 μM. But, overall biomass was reduced by around 25% in treatments with 50 μM risedronate (Fig. 7). Interestingly, total hydrocarbon content (pg•cell<sup>-1</sup>) was reduced in a dose dependent manner with total HBI content decreasing by 16% and 30% at risedronate treatments of 12.5 μM and 25 μM, respectively, compared to the control (Fig. 7). The HBI content of cells treated with 50 μM risedronate were not significantly different from those treated with 25 μM (Fig. 7). This amount can be attributed to HBIs produced during the pre-incubation period prior

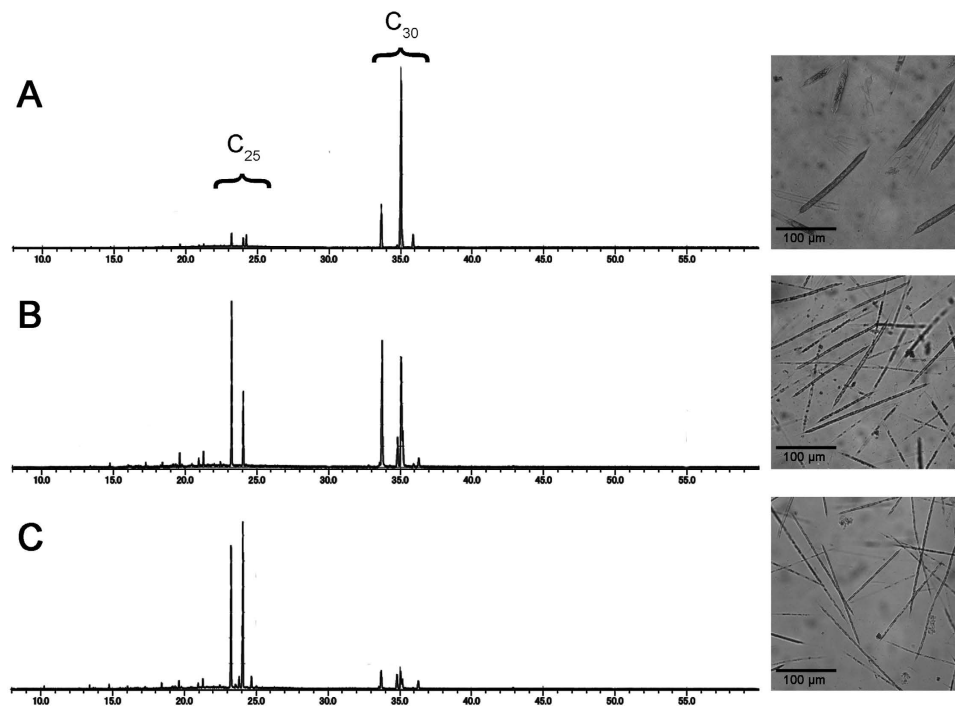


**Figure 8.** GC/MS total ion chromatograms of hydrocarbon extracts (left panels) and photomicrographs (right panels) of *R. setigera*. **A**) 1<sup>st</sup> culture cycle upon the onset of auxospore formation, **B**) 10<sup>th</sup> culture cycle after auxospore formation and **C**) 20<sup>th</sup> culture cycle after auxospore formation. Ion peaks appearing between 23 to 25 minutes were identified as C<sub>25</sub> HBIs and peaks appearing between 33 to 36 minutes were identified as C<sub>30</sub> HBIs based on comparisons of their mass spectra to *R. setigera* HBIs identified in previous studies.

Cycle	Cell Density (cells ml <sup>-1</sup> )	Cell Diameter (µm)	Relative Amounts of RsFPPS mRNA
Cy1	22,533 ± 1616 <sup>a</sup>	12.2 ± 0.6 <sup>a</sup>	1.00 ± 0.06 <sup>a</sup>
Cy10	80,400 ± 2400 <sup>b</sup>	6.1 ± 0.7 <sup>b</sup>	2.30 ± 0.26 <sup>b</sup>
Cy20	157,733 ± 4105 <sup>c</sup>	3.6 ± 0.6 <sup>c</sup>	6.55 ± 0.73 <sup>c</sup>

**Table 1.** Observed changes in culture cycles of *R. setigera* in relation to auxospore formation in terms of cell density, cell size (diameter), and relative amounts of RsFPPS mRNA. Values presented are the mean (± S.D.) of 3 replicate culture vessels for cell density, 60 measurements of individual cells for cell diameter, and 4 replicate wells for RsFPPS mRNA quantification by qPCR. Values under different superscripts denote significant differences ( $p < 0.05$ ).

to the addition of risedronate. These results would suggest that FPPS does contribute C<sub>15</sub> isoprenoids for HBI production in *R. setigera*.

**Changes in *R. setigera* hydrocarbon composition, cell morphology, and FPPS expression at different life cycle stages.** To monitor changes in the HBI composition of *R. setigera*, samples were collected for hydrocarbon analysis by GC/MS at the end of each 15 day culture period from the 1<sup>st</sup> (Cy1), 10<sup>th</sup> (Cy10) and 20<sup>th</sup> (Cy20) culture cycles after auxospore formation as representative samples of *R. setigera* at different stages of its life cycle. Significant changes in HBI composition were notably observed between cycles, wherein a shift from C<sub>30</sub> HBIs to C<sub>25</sub> HBIs as the major hydrocarbon component in cells was evident as culture cycles progressed after the auxospore formation event (Fig. 8A-C). Decreasing cell size and increasing cell densities were also noted in the succeeding culture cycles after auxospore formation (Table 1).

Measurement of relative RsFPPS mRNA levels for the corresponding culture cycles mentioned above was analyzed using RT-qPCR techniques with actin (RsACT) as a reference housekeeping gene for normalization. An increasing trend in RsFPPS mRNA levels was observed in succeeding culture cycles after auxospore formation with a 6-fold increase at Cy20 wherein cell density was highest and cell size was smallest (Table 1). Control experiments with reverse transcriptase omitted and replaced with nuclease free H<sub>2</sub>O

during cDNA synthesis gave no detectable signals by qPCR indicating the absence of genomic DNA in RNA preparations.

## Discussion

The use of bioinformatics has become a widely used and reliable tool for the discovery of functional genes. Through these techniques, we were able to screen two sets of *R. setigera* EST databases for a candidate FPPS. Using the information obtained from the EST databases to design gene specific primers, we were able to isolate an RsFPPS cDNA sequence spanning 1465 bp with an ORF of 1299 bp encoding a protein with 432 amino acids and an estimated molecular weight of 48.94 kDa.

The deduced amino acid sequence of RsFPPS cDNA had a high degree of similarity with other known FPP synthases<sup>20–22,27,29,30</sup>. In particular, the highly conserved domains I–VII as outlined by Koyama<sup>31</sup> were present in the RsFPPS protein. Domains II and VI contained highly conserved aspartate-rich motifs (DDxxD) that were determined to be essential for enzyme substrate binding and catalytic function. The first aspartate-rich motif (FARM) in domain II has been shown to play a role in determination of chain length for the resulting prenyl pyrophosphates through the presence of a conserved Phe residue located five amino acids upstream of the DDxxD motif<sup>32,33</sup>. Studies by Tarshis and co-workers<sup>34</sup> on the crystal structure of recombinant avian FPPS also revealed that the second aspartate-rich motif (SARM) in domain VI is the binding site for the homoallylic substrate IPP. Aside from FPP synthases, both FARM and SARM are also present in other *trans*-isoprenyl pyrophosphate synthases<sup>35</sup>. Enzyme assays carried out using the recombinant *E. coli* expressed and purified RsFPPS protein showed considerable enzyme activity and the formation of both FPP and GPP was observed using both LC/MS and GC/MS analyses. Taken together, these results strengthen our claim that the cDNA isolated in this study represents an FPPS gene from *R. setigera* and to our knowledge, is the first instance that an FPPS was cloned and characterized from a diatom.

The higher  $K_m$  values of RsFPPS for GPP compared to DMAPP as the allylic substrate were similar to those reported for FPPS of the trematode *Schistosoma mansoni*<sup>36</sup> and FDS-2 from the sagebrush *Artemisia tridentata*<sup>23</sup> that exhibited preference for DMAPP over GPP. Decreased enzyme activity observed at the highest concentrations of IPP used (200  $\mu$ M) in the enzyme assays (Fig. 5B,D) point to substrate inhibition typically observed for this enzyme with IPP beyond physiological concentrations<sup>37</sup>. The computed  $K_i$  values for these set of reactions revealed that the  $K_i$  for IPP was around two times higher in reactions with DMAPP compared to reactions with GPP (Fig. S5). Following the logic presented in previous studies<sup>38,39</sup> that showed substrate inhibition by high concentrations of IPP occurs due to the binding of IPP at the allylic site and that higher concentrations of the allylic substrate are necessary to counter this inhibiting effect, the higher  $K_i$  value of IPP for reactions with DMAPP further support the observation that RsFPPS exhibits a preference for DMAPP over GPP as an allylic substrate. In terms of turnover rate ( $k_{cat}$ ), comparison of reactions using GPP as the allylic substrate showed  $k_{cat}$  values that were on a scale 10-fold higher than those reported for the two FPPSs (FDS-1 and FDS-2) from *A. tridentata*<sup>23</sup>. Higher  $k_{cat}$  values for FPPS have only been reported from the phylogenetically distant bacteria *Bacillus stearothermophilus*<sup>40</sup> and show an interesting characteristic of RsFPPS (Supplementary Table 1). Given the high catalytic rates of RsFPPS observed in this study compared to those in literature, it stands as a potential candidate for heterologous expression in other model diatoms such as *Phaeodactylum tricorneratum*<sup>41,42</sup> which can be used as a platform in relation to efforts to engineer photosynthetic organisms for the production of valuable isoprenoids as biofuels, pharmaceuticals, cosmetics, or other compounds of interest.

GC/MS analysis of the corresponding reaction products after alkaline phosphatase treatment further revealed that RsFPPS also produced a small amount of the *cis*-isomers of GPP and *E,E*-FPP, namely NPP and *Z,E*-FPP, respectively. The formation of these *cis*-isomers tends to occur due to the balancing act that FPPS needs to achieve between proper double bond stereoselectivity of IPP and specific selectivity for IPP against its structural isomer DMAPP at the IPP binding site<sup>37</sup>. Although this phenomenon is not necessarily unique for FPPS as demonstrated in a study by Thulasiram and Poulter<sup>37</sup>, the presence of these *cis*-isomers may provide additional evidence for the hypothetical biosynthetic pathways for the various HBIs produced by *R. setigera* as proposed by Belt *et al.*<sup>12</sup> and Masse *et al.*<sup>11</sup>. Among the various HBIs from *R. setigera* characterized by Volkman *et al.*<sup>43</sup> and Rowland *et al.*<sup>9</sup>, structural *cis*- and *trans*-isomers at the T branching point of both C<sub>25</sub> and C<sub>30</sub> HBIs have been noted. This leads us to suggest the possibility that both the *cis*- and *trans*-prenyl pyrophosphates produced by RsFPPS could serve as precursors for these HBIs.

To test our hypothesis that RsFPPS provides the precursors necessary for HBI biosynthesis, we conducted *in vivo* inhibition experiments to assess whether FPPS inhibition would affect overall HBI production. Risedronate, a drug commonly used for bone resorption therapy, was determined to specifically target FPPS as its primary mode of action<sup>44–46</sup>. Using this drug, we were able to demonstrate that even at lower concentrations algal growth was not significantly affected, but HBI production was considerably impaired. These observations were similar to those made by Masse and co-workers<sup>10</sup> using mevinolin, an inhibitor of an upstream enzyme in the MVA pathway, 3-hydroxy-3-methylglutaryl-CoA reductase. Our results therefore point to the possible involvement of RsFPPS in the biosynthesis of HBIs in that inhibition of this enzyme potentially limits the amount of precursors necessary for subsequent HBI formation. Taking this into consideration further supports our argument regarding the involvement of RsFPPS in the proposed hypothetical biosynthetic pathway for HBIs previously put forth.



After demonstrating that RsFPPS produces potential precursors for HBIs, we tried to investigate whether RsFPPS played a regulatory role at the transcriptional level in the biosynthesis of varying types of HBIs produced by *R. setigera* throughout its life cycle. Based on initial observations of C<sub>30</sub> HBI predominance during the auxosporulation phase of *R. setigera*, we assumed that *R. setigera* would need more C<sub>15</sub> isoprenoid units produced by RsFPPS during this phase (Cy1) than during the phase when C<sub>25</sub> HBIs were predominant (Cy20). This assumption was also made based on various hypothetical biosynthetic pathways for HBIs proposed in previous studies<sup>11,12</sup>. Measurement of relative amounts of RsFPPS mRNA by RT-qPCR revealed that, contrary to our initial expectation that RsFPPS expression would be higher during auxosporulation due to the abundance of C<sub>30</sub> HBIs, RsFPPS mRNAs were actually more abundant during cycles when C<sub>25</sub> HBIs were predominant. This observation could be more in line with a function related to higher growth rates (i.e. faster cell division) rather than the regulation of the types of HBIs between life stages of *R. setigera*. The smaller cell size and higher cell densities observed in later culture cycles (when C<sub>25</sub> HBIs were predominant) are indicative of faster rates of cell division<sup>47</sup>. In the diatom *Phaeodactylum tricornutum*, increased protein production has been correlated with higher cell densities and faster growth rates<sup>48</sup>. Aside from proteins, sterols, which are derivatives of squalene produced from FPP, are important membrane components in eukaryotes<sup>49</sup> and sufficient amounts are needed during times of cell division<sup>50</sup>. Studies by Fabris and co-workers<sup>41</sup> also demonstrated that inhibition of sterol biosynthesis in diatoms was concomitant with reduced growth rates. Given the fact that FPP is located at a branch point in the isoprenoid biosynthetic pathway and is used for various other functions such as protein prenylation and sterol biosynthesis, it could be plausible to assume that the observed increases in RsFPPS mRNA levels are more of a function related to increased growth rates and have little or no regulatory role in terms of the types of hydrocarbons produced by *R. setigera* at various life stages. Furthermore, the relatively small amounts of HBIs produced by *R. setigera* (roughly <1% dry weight) and the nearly similar ratios between their *cis*- and *trans*- isomers<sup>9</sup> may indicate that it only uses a small fraction of the pool of *E,E*-FPP and GPP to produce the HBIs.

In summary, we have isolated and characterized a cDNA that encodes a functional farnesyl pyrophosphate synthase from the marine diatom *R. setigera*. In our attempts to better understand how this diatom produces unique HBIs, we have presented several lines of evidence that point to the possible contribution of RsFPPS in overall HBI biosynthesis. In terms of the regulation of the types of HBIs produced by *R. setigera* throughout its life cycle though, RsFPPS does not seem to play any significant role and this phenomenon is most likely controlled by a different set of enzymes which can probably use both the *cis*- and *trans*- forms of GPP and FPP as substrates. We are therefore currently undertaking additional studies to discover tentative enzymes from *R. setigera* that can catalyze the final formation of these HBIs.

## Methods

**Algal culture.** *Rhizosolenia setigera* CCMP1694 was obtained from the National Center for Marine Algae and Microbiota (Maine, USA). Cultures of *R. setigera* were maintained in 300 ml of f/2 medium<sup>51</sup> in 500 ml Erlenmeyer flasks under controlled conditions (25 °C, illumination at 250 μmol photons m<sup>-2</sup> s<sup>-1</sup>, 12:12 light:dark cycle). Culture cycles were carried out over a period of 15 days and after each culture cycle, 50 ml of 15 day-old culture was used to inoculate 250 ml of fresh f/2 medium. All culture cycles were carried out in triplicate. To determine the effect of auxosporulation on the hydrocarbon production and FPPS gene expression levels, cultures were constantly monitored by light microscopy for the onset of auxosporulation as determined by morphological changes (i.e. larger cell diameters). In the initial culture cycle when the onset of auxosporulation was notably observed (denoted as Cycle 1), aliquotes of 100 ml were collected on Whatman GF/C glass filters (GE Healthcare, United Kingdom) by vacuum filtration, freeze-dried for 24 hours, and stored for hydrocarbon extraction and analysis. The rest of the culture was collected on a 20 μm plankton net and the harvested algal cells were snap frozen with liquid nitrogen, and stored at -80 °C for RNA extraction and expression analysis. Similar samplings were carried out in succeeding culture cycles.

**Hydrocarbon extraction.** The hydrocarbon fraction from *R. setigera* was obtained from the freeze-dried samples collected on GF/C filters by extraction following methods previously reported<sup>52</sup>. The resulting hydrocarbon fraction was subsequently concentrated with a rotary evaporator and a 2.5 μl portion was subjected to GC/MS analysis under conditions described below.

**RsFPPS cDNA cloning.** A cDNA library was prepared from RNA extracted from 6 day-old *R. setigera* cells cultured under the same conditions mentioned above. Total RNA was extracted with TRIzol (Invitrogen, Carlsbad, CA) and mRNA was purified using Oligotex<sup>TM</sup>-dT<sub>30</sub> Super mRNA Purification Kit (Takara, Shiga, Japan). ZAP Express cDNA Synthesis Kit and Gigapack III Gold Cloning Kit (Agilent, Santa Clara, CA) were used for cDNA synthesis and library construction according to the manufacturer's instructions. The original library composed of 200,000 clones was amplified once in XL 1-Blue MRF<sup>+</sup> *E. coli* cells (Agilent).

A putative nucleotide sequence encoding FPPS was mined from two independent *R. setigera* expressed sequence tag (EST) databases by inputting queries of other known sequences for FPPS using the local BLAST function in BioEdit V 7.2.3<sup>53</sup>. From each database, single contigs with high similarity to other FPP synthases were identified. One contig corresponded to 1545 bp while the other contig was 1474 bp

long. Both contigs contained a putative open reading frame (ORF) corresponding to 1299 bp (RsFPPS) encoding 432 amino acid residues with 100% identity with each other. To confirm this sequence, the forward primer Rs-FPPS-est-F and reverse primer Rs-FPPS-est-R (Supplementary Table 2) were designed to amplify a fragment of 1465 bp that included the entire putative coding region and portions of the 5' and 3' untranslated regions (UTR) for FPPS. PCR amplification was carried out using KOD DNA polymerase (Toyobo Co. Ltd., Osaka, Japan) and the constructed cDNA library as template. The PCR product was purified by agarose gel electrophoresis and ligated to the EcoRV site of the plasmid pBluescript II KS+ (Agilent). The resulting plasmid was designated as pBs-RsFPPS1465 and transformed into XL 1-Blue MRF<sup>+</sup> *E. coli* cells (Agilent) by the standard CaCl<sub>2</sub> protocol. The transformants were plated following protocols for standard blue-white colony selection. Independent positive white colonies were selected to purify plasmids containing the insert for confirmation by sequencing.

**Phylogenetic analysis.** The deduced amino acid sequence of RsFPPS was compared to the sequences of other known FPPSs using BLAST<sup>54</sup>. Sequence alignment was carried out using CLUSTAL W<sup>55,56</sup> against characterized representative sequences from mouse (*Mus musculus*)<sup>27</sup>, yeast (*Saccharomyces cerevisiae*)<sup>20</sup>, bacteria (*Bacillus stearothermophilus*)<sup>30</sup>, and the higher plants *Lupinus albus*<sup>21</sup>, *Arabidopsis thaliana*<sup>22</sup>, and *Zea mays*<sup>29</sup>. A phylogenetic tree was constructed using the Neighbor Joining function on MEGA software version 4.0<sup>57–59</sup> using the sequences mentioned above along with additional characterized or annotated FPPS sequences from human<sup>28</sup>, avian<sup>34</sup>, piscine<sup>60</sup>, algal<sup>61–63</sup> and yeast<sup>64</sup> sources.

**Enzyme assay.** Recombinant RsFPPS protein expression and purification are detailed in *Supplementary Methods*. The purified enzyme's activity was assayed using methods patterned after those previously described<sup>21</sup>. Unless otherwise stated, reactions were carried out in 1.5 ml Eppendorf tubes in a total volume of 100  $\mu$ l containing 35 mM Tris-HCl (pH 7.5), 10 mM MgCl<sub>2</sub>, 4 mM dithiothreitol (DTT), 50  $\mu$ M isopentenyl pyrophosphate (IPP; Sigma-Aldrich, St. Louis, MO), 150  $\mu$ M dimethylallyl pyrophosphate (DMAPP; Sigma) or geranyl pyrophosphate (GPP; Sigma) as the allylic substrates, and 100 ng of the purified enzyme. Assay mixtures were prepared in bulk without the substrates and the reactions were initiated by substrate addition after sufficient equilibration of the system temperature. For enzyme kinetic analysis, concentrations of the allylic substrates were varied ranging from 5–200  $\mu$ M. Parallel assays were done with the allylic substrates at a constant concentration (50  $\mu$ M DMAPP or 100  $\mu$ M GPP) and IPP as the counter substrate. Reactions were carried out at 30 °C for 10 minutes and stopped by snap freezing the assay tubes in liquid nitrogen. To denature and precipitate the proteins prior to LC/MS analysis, 100  $\mu$ l of acetonitrile was added to the mixture, vortexed for 10 seconds, and centrifuged at 19,000 g for 5 minutes at 4 °C. Detailed analysis and identification of reaction products by GC/MS were carried following the methods of Thulasiram and Poulter<sup>37</sup>.

**Identification and quantification of assay products by LC/MS.** Identification of assay products and analysis of enzyme activity were patterned after modified methods of Nagel *et al.*<sup>65</sup> and Zhang and Poulter<sup>66</sup>. Analysis was carried out on a Shimadzu LC-20AD HPLC system (Shimadzu, Kyoto, Japan) coupled to an AmaZon SL ion trap mass spectrometer (Bruker Daltonics, USA). Separation of reaction products (GPP and FPP) was achieved on an Inertsil ODS-3 column (particle size 3  $\mu$ m, 4.6 mm ID x 50 mm, GL Sciences, Tokyo, Japan) using a mobile phase consisting of 5 mM NH<sub>4</sub>HCO<sub>3</sub> as solvent A and 100% acetonitrile as solvent B. A gradient system starting at 0% solvent B, 100% solvent A and increasing to 100% solvent B, 0% solvent A in 8 minutes and a hold at 100% solvent B for an additional 2 minutes was used. A change to 0% solvent B held for 2.5 minutes was done prior to the next injection. Flow rate was at 0.8 ml min<sup>-1</sup>, column temperature set at 40 °C, and injection volume set at 10  $\mu$ l for all samples and standards. The mass spectrometer was set in negative electrospray ionization mode with ion spray voltage set at -4500 V. For more precise quantification, multiple reaction monitoring was done with transitions of *m/z* 313.4/159.0 for GPP and *m/z* 381.5/159.0 for FPP. To establish calibration curves, FPP and GPP standards (Sigma) were prepared and diluted in the same sample matrix used for enzyme assays. Enzyme activity was computed as the amount of FPP produced per minute per mg of protein. Data analysis was done on DataAnalysis V1.5 and QuantAnalysis V1.3.2 software (Bruker Daltonics). Graphs and statistical analysis for enzyme kinetics were done using GraphPad PRISM software V 6.0 (GraphPad Software Inc., La Jolla, CA, USA).

**GC/MS analysis.** Algal hydrocarbon extracts and the corresponding prenyl alcohols obtained by enzymatic dephosphorylation of the enzyme reaction products were analyzed by GC/MS based on methods previously reported<sup>52</sup>. Identification of algal hydrocarbons was based on relative retention times and mass spectra of previously characterized HBIs from *R. setigera* while identification of enzyme reaction products was based on their relative retention times and mass spectra of prenyl alcohols in the mass spectra library on the Shimadzu GCMS LabSolution software V 2.71.

**In vivo inhibition of RsFPPS with risedronate.** For inhibition studies with risedronate (Tokyo Chemical Industry, Tokyo, Japan), algal cultures fifteen cycles after auxosporeulation were used. Using the same conditions mentioned above, a 1L cell culture was allowed to grow for 4 days and subsequently subdivided into 60 ml aliquotes in 100 ml erlenmeyer flasks upon which risedronate was added at concentrations

of 0, 12.5, 25, and 50  $\mu\text{M}$ . Each treatment was done in triplicate. The cultures were then allowed to incubate for an additional two days before 50 ml was collected on GF/C glass filters for hydrocarbon analysis.

For quantitative analysis of hydrocarbons in risedronate treated cultures, 10 ng of hexadecane was added to each filter paper as an internal standard prior to extraction and a 2  $\mu\text{l}$  portion was used for GC/MS analysis. Quantification was done by creating a calibration curve using an authentic  $\text{C}_{25}$  HBI isomer isolated from *R. setigera* as a standard.

**RsFPPS gene expression analysis by RT-qPCR.** The relative expression levels of RsFPPS were monitored in cultures of *R. setigera* at various stages in its life cycle. Total RNA was extracted from diatom samples stored at  $-80^\circ\text{C}$  as described above. cDNA synthesis for qPCR was done using iScript cDNA Synthesis Kit (Bio-Rad) following the manufacturer's protocols. qPCR reaction mixtures contained 10  $\mu\text{l}$  of SsoFast EvaGreen Supermix (Bio-Rad), 7  $\mu\text{l}$  of PCR-grade water, 1  $\mu\text{l}$  each of forward and reverse primers (10  $\mu\text{M}$ ), and 1  $\mu\text{l}$  of the synthesized cDNA for a total volume of 20  $\mu\text{l}$ . Monitoring of real-time PCR reactions was done on a CFX96 Real-Time System coupled to a C1000 Thermal Cycler (Bio-Rad). Relative expression levels of RsFPPS were normalized against the actin gene (RsACT) as a reference housekeeping gene<sup>67</sup>. Primers for RsFPPS were designed from the confirmed sequence of plasmid pBs-RsFPPS1465 while primers for RsACT were designed based on similar contigs mined from the two *R. setigera* EST databases mentioned earlier (Supplementary Table 2). To test for contamination of genomic DNA, extracted RNA was subjected to similar methods mentioned above with the exception that reverse transcriptase was replaced with nuclease free  $\text{H}_2\text{O}$  in the cDNA synthesis step. The nucleotide sequences for RsFPPS and RsACT have been submitted to the NCBI GenBank™ database with accession numbers KM360174 and KM360175 respectively.

## References

- Mann, D. G. & Vanormelingen, P. An inordinate fondness? The number, distributions, and origins of diatom species. *J. Eukaryot. Microbiol.* **60**, 414–420 (2013).
- Gao, K. *et al.* Rising  $\text{CO}_2$  and increased light exposure synergistically reduce marine primary productivity. *Nature Clim. Change* **2**, 519–523 (2012).
- Sinninghe Damste, J. S. *et al.* The rise of rhizosolenid diatoms. *Science* **304**, 584–587 (2004).
- Rowland, S. J. & Robson, J. N. The widespread occurrence of highly branched acyclic  $\text{C}_{20}$ ,  $\text{C}_{25}$  and  $\text{C}_{30}$  hydrocarbons in recent sediments and biota - A review. *Mar. Environ. Res.* **30**, 191–216 (1990).
- Rowland, S. J., Belt, S. T., Masse, G., Roussakis, C. & Robert, J.-M. Effects of temperature on polyunsaturation in cytosolic lipids of *Haslea ostrearia*. *Phytochemistry* **56**, 597–602 (2001).
- Melis, A. Photosynthesis-to-fuels: from sunlight to hydrogen, isoprene, and botryococcene production. *Energy Environ. Sci.* **5**, 5531–5539 (2012).
- Hillen, L. W., Pollard, G., Wake, L. V. & White, N. Hydrocracking of the oils of *Botryococcus braunii* to transport fuels. *Biotechnol. Bioeng.* **24**, 193–205 (1982).
- Belt, S. T., Allard, W. G., Robert, J.-M., Rowland, S. J. Effects of auxospore formation on distributions of  $\text{C}_{25}$  and  $\text{C}_{30}$  isoprenoid alkenes in *Rhizosolenia setigera*. *Phytochemistry* **59**, 141–148 (2002).
- Rowland, S. J. *et al.* Factors influencing the distributions of polyunsaturated terpenoids in the diatom, *Rhizosolenia setigera*. *Phytochemistry* **58**, 717–728 (2001).
- Masse, G., Belt, S. T. & Rowland, S. J. & Rohmer, M. Isoprenoid biosynthesis in the diatoms *Rhizosolenia setigera* (Brightwell) and *Haslea ostrearia* (Simonsen). *Proc. Natl. Acad. Sci. USA* **101**, 4413–4418 (2004).
- Masse, G., Belt, S. T. & Rowland, S. J. Biosynthesis of unusual monocyclic alkenes by the diatom, *Rhizosolenia setigera* (Brightwell). *Phytochemistry* **65**, 1101–1106 (2004).
- Belt, S. T., Masse, G., Rowland, S. J. & Rohmer, M. Highly branched isoprenoid alcohols and epoxides in the diatom *Haslea ostrearia* Simonsen. *Org. Geochem.* **37**, 133–145 (2006).
- Dhar, M. K., Koul, A. & Kaul, S. Farnesyl pyrophosphate synthase: a key enzyme in isoprenoid biosynthetic pathway and potential molecular target for drug development. *N. Biotechnol.* **30**, 114–123 (2013).
- Pandit, J. *et al.* Crystal structure of human squalene synthase. A key enzyme in cholesterol biosynthesis. *J. Biol. Chem.* **275**, 30610–30617 (2000).
- Starks, C. M., Back, K., Chappell, J. & Noel, J. P. Structural basis for cyclic terpene biosynthesis by tobacco 5-epi-aristolochene synthase. *Science* **277**, 1815–1820 (1997).
- Schnee, C. *et al.* The products of a single maize sesquiterpene synthase form a volatile defense signal that attracts natural enemies of maize herbivores. *Proc. Natl. Acad. Sci. USA* **103**, 1129–1134 (2006).
- Clarke, S. Protein isoprenylation and methylation at carboxyl-terminal cysteine residues. *Annu. Rev. Biochem.* **61**, 355–386 (1992).
- Wilkin, D. J., Kutsunai, S. Y. & Edwards, P. A. Isolation and sequence of the human farnesyl pyrophosphate synthetase cDNA. *J. Biol. Chem.* **265**, 4607–4614 (1990).
- Clarke, C. F. *et al.* Molecular cloning and sequence of a cholesterol-repressible enzyme related to prenyltransferase in the isoprene biosynthetic pathway. *Mol. Cell. Biol.* **7**, 3138–3146 (1987).
- Anderson, M. S., Yarger, J. G., Burck, C. L. & Poulter, C. D. Farnesyl diphosphate synthetase. Molecular cloning, sequence, and expression of an essential gene from *Saccharomyces cerevisiae*. *J. Biol. Chem.* **264**, 19176–19184 (1989).
- Attucci, S., Aitken, S. M., Gulick, P. J. & Ibrahim, R. K. Farnesyl pyrophosphate synthase from white lupin: molecular cloning, expression, and purification of the expressed protein. *Arch. Biochem. Biophys.* **321**, 493–500 (1995).
- Delourme, D., Lacroute, F. & Karst, F. Cloning of an *Arabidopsis thaliana* cDNA coding for farnesyl diphosphate synthase by functional complementation in yeast. *Plant Mol. Biol.* **26**, 1867–1873 (1994).
- Hemmerlin, A., Rivera, S. B., Erickson, H. K. & Poulter, C. D. Enzymes encoded by the farnesyl diphosphate synthase gene family in the Big Sagebrush *Artemisia tridentata* ssp. *spiciformis*. *J. Biol. Chem.* **278**, 32132–32140 (2003).
- Pilsyk, S. *et al.*, Overexpression of erg20 gene encoding farnesyl pyrophosphate synthase has contrasting effects on activity of enzymes of the dolichyl and sterol branches of mevalonate pathway in *Trichoderma reesei*. *Gene* **544**, 114–122 (2014).
- Ling, Y., Li, Z. -H., Miranda, K., Oldfield, E. & Moreno, S. N. J. The farnesyl-diphosphate/geranylgeranyl-diphosphate synthase of *Toxoplasma gondii* is a bifunctional enzyme and a molecular target of bisphosphonates. *J. Biol. Chem.* **282**, 30804–30816 (2007).

26. Masferrer, A. *et al.* Overexpression of *Arabidopsis thaliana* farnesyl diphosphate synthase (FPS1S) in transgenic *Arabidopsis* induces a cell death/senescence-like response and reduced cytokinin levels. *Plant J.* **30**, 123–132 (2002).
27. Andalibi, A. *et al.* Mapping of multiple mouse loci related to the farnesyl pyrophosphate synthase gene. *Mammal. Genome* **4**, 211–219 (1993).
28. Sheares, B. T. *et al.* Cloning, analysis, and bacterial expression of human farnesyl pyrophosphate synthetase and its regulation in Hep G2 cells. *Biochemistry* **28**, 8129–8135 (1989).
29. Li, C. P. & Larkins B. A. Identification of a maize endosperm-specific cDNA encoding farnesyl pyrophosphate synthetase. *Gene* **171**, 193–196 (1996).
30. Koyama, T. *et al.* Thermostable farnesyl diphosphate synthase of *Bacillus stearothermophilus*: molecular cloning, sequence determination, overproduction, and purification. *J. Biochem.* **113**, 355–363 (1993).
31. Koyama, T. Molecular analysis of prenyl chain elongating enzymes. *Biosci. Biotechnol. Biochem.* **63**, 1671–1676 (1999).
32. Ohnuma, S. -I. *et al.* Conversion of product specificity of archaeobacterial geranylgeranyl-diphosphate synthase, identification of essential amino acid residues for chain length determination of prenyltransferase reaction. *J. Biol. Chem.* **271**, 18831–18837 (1996).
33. Tarshis, L. C., Proteau, P. J., Kellogg, B. A., Sacchettini, J. C. & Poulter, C. D. Regulation of product chain length by isoprenyl diphosphate synthases. *Proc. Natl. Acad. Sci. USA* **93**, 15018–15023 (1996).
34. Tarshis, L. C., Yan, M., Poulter, C. D. & Sacchettini, J. C. Crystal structure of recombinant farnesyl diphosphate synthase at 2.6-Å resolution. *Biochemistry* **33**, 10871–10877 (1994).
35. Liang, P. -H., Ko, T. -P. & Wang, A. H. -J. Structure, mechanism and function of prenyltransferases. *Eur. J. Biochem.* **269**, 3339–3354 (2002).
36. Ziniel, P. D. *et al.* Characterization of potential drug targets farnesyl diphosphate synthase and geranylgeranyl diphosphate synthase in *Schistosoma mansoni*. *Antimicrob. Agents Chemother.* **57**, 5969–5976 (2013).
37. Thulasiram, H. V. & Poulter, C. D. Farnesyl diphosphate synthase: the art of compromise between substrate selectivity and stereoselectivity. *J. Am. Chem. Soc.* **128**, 15819–15823 (2006).
38. Laskovics, F. M., Krafcik, J. M. & Poulter, C. D. Prenyltransferase. Kinetic studies of the 1'-4 coupling reaction with avian liver enzyme. *J. Biol. Chem.* **254**:9458–9463 (1979).
39. Reed, B. C., Rilling, H. C. Substrate binding of avian liver prenyltransferase. *Biochemistry* **15**:3739–3745 (1976).
40. Koyama, T. *et al.* Identification of significant residues in the substrate binding site of *Bacillus stearothermophilus* farnesyl diphosphate synthase. *Biochemistry* **35**, 9533–9538 (1996).
41. Fabris, M. *et al.* Tracking the sterol biosynthesis pathway of the diatom *Phaeodactylum tricornutum*. *New Phytol.* (2014) DOI: 10.1111/nph.12917.
42. Apt, K. E., Grossman, A. R. & Kroth-Pancic, P. G. Stable nuclear transformation of the diatom *Phaeodactylum tricornutum*. *Mol. Gen. Genet.* **252**, 572–579 (1996).
43. Volkman, J. K., Barrett, S. M. & Dunstan, G. A. C<sub>25</sub> and C<sub>30</sub> highly branched isoprenoid alkenes in laboratory cultures of two marine diatoms. *Org. Geochem.* **21**, 407–413 (1994).
44. van Beek, E., Pieterman, E., Cohen, L., Löwik, C. & Papapoulos, S. Farnesyl pyrophosphate synthase is the molecular target of nitrogen-containing bisphosphonates. *Biochem. Biophys. Res. Commun.* **264**, 108–111 (1999).
45. Montalvetti, A. *et al.* Bisphosphonates are potent inhibitors of *Trypanosoma cruzi* farnesyl pyrophosphate synthase. *J. Biol. Chem.* **276**, 33930–33937 (2001).
46. Ebetino, F. H. *et al.* Molecular interactions of nitrogen-containing bisphosphonates within farnesyl diphosphate synthase. *J. Organomet. Chem.* **690**, 2679–2687 (2005).
47. Montagnes, D. J. S. & Franklin, D. J. Effect of temperature on diatom volume, growth rate, and carbon and nitrogen content: Reconsidering some paradigms. *Limnol. Oceanogr.* **46**, 2008–2018 (2001).
48. Chrismadha, T. & Borowitzka, M. A. Effect of cell density and irradiance on growth, proximate composition and eicosapentaenoic acid production of *Phaeodactylum tricornutum* grown in a tubular photobioreactor. *J. Appl. Phycol.* **6**, 67–74 (1994).
49. Volkman, J. K. Sterols in microorganisms. *Appl. Microbiol. Biotechnol.* **60**, 495–506 (2003).
50. Boutte, Y. & Grebe, M. Cellular processes relying on sterol function in plants. *Curr. Opin. Plant Biol.* **12**, 705–713 (2009).
51. Guillard, R. R. L. & Ryther, J. H. Studies of marine planktonic diatoms. I. *Cyclotella nana* Hustedt, and *Detonula confervacea* (Cleve) Gran. *Can. J. Microbiol.* **8**, 229–239 (1962).
52. Okada, S., Murakami, M. & Yamaguchi, K. Hydrocarbon composition of newly isolated strains of the green microalga *Botryococcus braunii*. *J. Appl. Phycol.* **7**, 555–559 (1995).
53. Hall, T. A. BioEdit: a user-friendly biological sequence alignment editor and analysis program for Windows 95/98/NT. *Nucleic Acids Symp. Ser.* **41**, 95–98 (1999).
54. Altschul, S. F., Gish, W., Miller, W., Myers, E. W. & Lipman, D. J. Basic local alignment search tool. *J. Mol. Biol.* **215**, 403–410 (1990).
55. Larkin, M. A. *et al.* Clustal W and Clustal X version 2.0. *Bioinformatics* **23**, 2947–2948 (2007).
56. Goujon, M. *et al.* A new bioinformatics analysis tools framework at EMBL-EBI. *Nucleic Acids Res.* **38**, W695–W699 (2010).
57. Saitou, N. & Nei, M. The neighbor-joining method: a new method for reconstructing phylogenetic trees. *Mol. Biol. Evol.* **4**, 406–425 (1987).
58. Zuckerkandl, E. & Pauling, L. [Evolutionary divergence and convergence in proteins] *Evolving Genes and Proteins* [Bryson, V. & Vogel, H.J. (eds.)] [97–166] (Academic Press, New York, 1965).
59. Tamura, K., Dudley, J., Nei, M., Kumar, S. MEGA4: Molecular Evolutionary Genetics Analysis (MEGA) software version 4.0. *Mol. Biol. Evol.* **24**, 1596–1599 (2007).
60. Woods, I. G. *et al.* The zebrafish gene map defines ancestral vertebrate chromosomes. *Genome Res.* **15**, 1307–1314 (2005).
61. Merchant, S. S. *et al.* The Chlamydomonas genome reveals the evolution of key animal and plant functions. *Science* **318**, 245–250 (2007).
62. Cock, J. M. *et al.* The Ectocarpus genome and the independent evolution of multicellularity in brown algae. *Nature* **465**, 617–621 (2010).
63. Corteggiani Carpinelli, E. *et al.* Chromosome scale genome assembly and transcriptome profiling of *Nannochloropsis gaditana* in nitrogen depletion. *Mol. Plant* **7**, 323–335 (2014).
64. Ma, L. J. *et al.* Genomic analysis of the basal lineage fungus *Rhizopus oryzae* reveals a whole-genome duplication. *PLoS Genet.* **5**, E1000549 (2009).
65. Nagel, R., Gershenzon, J., & Schmidt, A. Nonradioactive assay for detecting isoprenyl diphosphate synthase activity in crude plant extracts using liquid chromatography coupled with tandem mass spectrometry. *Anal. Biochem.* **422**, 33–38 (2012).
66. Zhang, D. L. & Poulter, C. D. Analysis and purification of phosphorylated isoprenoids by reversed-phase HPLC. *Anal. Biochem.* **213**, 356–361 (1993).
67. Siat, M. *et al.* Molecular toolbox for studying diatom biology in *Phaeodactylum tricornutum*. *Gene* **406**, 23–35 (2007).

## Acknowledgments

We thank T. Yoshimatsu for preparation of *Rhizosolenia* cultures. We are grateful to Y. Ohnishi and K. Fukunaga for preparation of total RNA of *Rhizosolenia setigera*. The encouragement from and discussions with Dr. H. Uchida are also appreciated. This study was supported by the New Energy and Industrial Technology Development Organization (NEDO), Japan, under the program “Strategic Development of Next Generation Bioenergy Utilization Technology”.

## Author Contributions

V.M.E.F., R.Y. and K.T. performed the experiments. V.M.E.F. and S.O. designed the study and wrote the manuscript. M.A. contributed the EST database and reviewed the manuscript. K.T. and S.M. provided technical discussions and reviewed the manuscript.

## Additional Information

**Supplementary information** accompanies this paper at <http://www.nature.com/srep>

**Competing financial interests:** The authors declare no competing financial interests.

**How to cite this article:** Ferriols, V. M. E. N. *et al.* Cloning and characterization of farnesyl pyrophosphate synthase from the highly branched isoprenoid producing diatom *Rhizosolenia setigera*. *Sci. Rep.* **5**, 10246; doi: 10.1038/srep10246 (2015).



This work is licensed under a Creative Commons Attribution 4.0 International License. The images or other third party material in this article are included in the article's Creative Commons license, unless indicated otherwise in the credit line; if the material is not included under the Creative Commons license, users will need to obtain permission from the license holder to reproduce the material. To view a copy of this license, visit <http://creativecommons.org/licenses/by/4.0/>